EFDA–JET–PR(12)27

A. Murari, P. Boutot, J. Vega, M. Gelfusa, R. Moreno, G. Verdoolaege,
P.C. de Vries and JET EFDA contributors

Clustering Based on the Geodesic Distance on Gaussian Manifolds for the Automated Classification of Disruptions

Clustering Based on the Geodesic Distance on Gaussian Manifolds for the Automated Classification of Disruptions

A. Murari[1], P. Boutot[2], J. Vega[3], M. Gelfusa[4], R. Moreno[3], G. Verdoolaege[5], P.C. de Vries[6] and JET EFDA contributors*

JET-EFDA, Culham Science Centre, OX14 3DB, Abingdon, UK

[1]Consorzio RFX-Associazione EURATOM ENEA per la Fusione, I-35127 Padova, Italy
[2]Ecole Polytechnique de Palaiseau, Paris, France
[3]Asociación EURATOM/CIEMAT para Fusión. Avda. Complutense, 22. 28040 Madrid, Spain
[4]Associazione EURATOM-ENEA - University of Rome "Tor Vergata", Roma, Italy
[5]Department of Applied Physics, Ghent University, Ghent, Belgium
[6]FOM institute DIFFER, Association EURATOM-FOM, PO Box 1207, 3430BE Nieuwegein, The Netherlands
** See annex of F. Romanelli et al, "Overview of JET Results", (23rd IAEA Fusion Energy Conference, Daejon, Republic of Korea (2010)).*
** See annex of F. Romanelli et al, "Overview of JET Results", (24th IAEA Fusion Energy Conference, San Diego, USA (2012)).*

Preprint of Paper to be submitted for publication in
Nuclear Fusion

“This document is intended for publication in the open literature. It is made available on the understanding that it may not be further circulated and extracts or references may not be published prior to publication of the original when applicable, or without the consent of the Publications Officer, EFDA, Culham Science Centre, Abingdon, Oxon, OX14 3DB, UK.”

“Enquiries about Copyright and reproduction should be addressed to the Publications Officer, EFDA, Culham Science Centre, Abingdon, Oxon, OX14 3DB, UK.”

The contents of this preprint and all other JET EFDA Preprints and Conference Papers are available to view online free at www.iop.org/Jet. This site has full search facilities and e-mail alert options. The diagrams contained within the PDFs on this site are hyperlinked from the year 1996 onwards.

ABSTRACT

In the last years progress has been made on the front of disruption prediction in Tokamaks. The less forgiving character of the new metallic walls at JET emphasized the importance of disruption prediction and mitigation. Being able not only to predict but also classify the type of disruption will enable to better choose the appropriate mitigation strategy. In this perspective, a new clustering method, based on the geodesic distance on a probabilistic manifold, has been applied to the JET disruption database. This approach allows taking into account the error bars of the measurements and has proved to clearly outperform the more traditional classification methods based on the Euclidean distance. The developed technique with the highest success rate manages to identify the type of disruption with 85% confidence several hundreds of ms before the thermal quench. Therefore the combined use of this method and the more traditional disruption predictors would improve significantly the mitigation strategy on JET and could contribute to the definition of an optimised approach for ITER.

1. DISRUPTIONS AND OPERATIONAL LIMITS

Disruptions are a sudden loss of confinement that results in the abrupt termination of the plasma discharge and can lead to damage to the tokamak [1]. Disruptions usually consist of several phases: the first is called thermal quench during which a large fraction of the plasma thermal energy is released in a short interval of the order of a few ms. The second phase of the disruption is called the current quench, in which the plasma current rapidly decays to zero. In this second phase, the vertical stability of the plasma is often compromised, leading to Vertical Displacement Events (VDE): a sudden movement of the plasma in the vertical direction. During disruptions a large fraction of the plasma kinetic and magnetic energy can be deposited on the plasma facing components (PFC). Moreover large electromagnetic forces are exerted on the surrounding conductors including the vacuum vessel. A fast current quench with high internal inductance can also cause high negative loop voltages and can lead to production of relativistic "runaway electrons" [2]. These relativistic electrons in their turn are potentially very dangerous since they can cause severe damage to the PFC and also to the tokamak first wall. It is estimated that almost 70% of the initial plasma current can be converted into runaways during a disruption or fast current quench in ITER [3].

One of the main problems with disruptions is that their potential danger increases with the size of the devices; minor damage in present tokamaks can translate into major integrity issues in the next generation of devices such as ITER. Moreover, disruptions are unavoidable in current tokamaks, although the disruption rate during JET last campaigns with the carbon wall was limited to 3.4% [4]. On the other hand with the new ITER-like Wall (ILW) the disruptivity rate has increased to about 8% [5] and similar values can be envisaged for the initial operation of ITER. Hence, improvement of disruption and mitigation strategies is of the highest importance.

From a physics point of view, the non-linear nature of disruptions makes it a phenomenon that is difficult to study and to model. The root causes can reside in a multitude of instabilities and/or

failures of the control systems [6, 4]. The evolution of disruptions is also believed to be affected by the electromagnetic properties of the devices. All these issues have frustrated so far the development of theoretical models capable of predicting the occurrence of disruptions. In the last decade, therefore, a lot of efforts have been devoted to the developments of predictors based on machine learning tools.

In most early experiments, the prediction was based on monitoring one or two basic signals [7]; locked modes or global plasma energy. The alarm trigger was started when these signals crossed some appropriate threshold. The problem of these methods is the limited potential to detect disruptions in different plasma configurations and at the same time achieve low false alarm rates. Another possibility is to use neural networks (NN) with multiple diagnostics as inputs. The neural network output can be trained to predict the time to the disruption [8] or a number proportional to the probability of the disruption. Usually, an appropriate threshold is also selected to launch an alarm. For example a NN to predict the density-limit disruptions was developed for ASDEX Upgrade [9]. The inputs were 13 parameters and the alarm was to be triggered 50 ms before the predicted onset of the disruption. The database to train these networks contained 99 disruptive and 386 non-disruptive shots. They reached 15% missed rate on 65 disruptions and 1% false alarm rate for 500 non-disruptive shots. In JT-60 also a NN with 9 inputs was used [10]. The NN was trained with 12 disruptive and 6 non-disruptive shots that were manually selected and manually classified to determine different stability levels. The results were 97% success rate 10 ms in advance for 300 disruptive shots with 2.1% false alarm rate for 1008 non-disruptive shots. Other approaches, relying on more advanced tools such as Fuzzy Logic, have also been tested [11].

However, most of the current articles in the literature are focused only on the proof of principle of the various techniques. Actual real-time deployment of these techniques is not performed. On JET a new predictor, called the Advanced Predictor Of DISruptions (APODIS), has been recently developed and was actually deployed in real-time during the last campaigns with the ILW [12]. It consists of a combination of supervised classification systems, based on SVM (Support Vector Machines) organised in two layers. The first layer contains a series of three different SVM predictors, analysing three consecutive time windows (each one 32ms long) of data to take into account the history of the discharge. The outputs of these three evaluations are used as inputs to the second layer classifier, which takes the decision whether or not to launch an alarm. APODIS has been conceived to run in real-time, and indeed it has been deployed in JET real-time system during the last campaigns with the new ILW [13]. Practically all the 305 disruptions, which occurred during the period APODIS was active, were detected: the five missed were due to the limited time resolution of the implemented version of APODIS (32ms). The number of false alarms is also very low and typically due to problems with the signals used as inputs (which is an important issue but which should be attacked at the level of individual diagnostic systems). Also the various mitigation tools, the fast valve for massive gas injection, and the strategies of the plasma landing have proved to be quite effective in reducing the detrimental effects of the disruptions on the plasma facing components and the vacuum vessel [5, 14].

Disruptions can be quite different in nature, both from the point of view of the root causes as in the further evolution. The description of the physics behind the various types of disruptions is not the subject of this paper. A brief overview of the main operational limits is given in the following to illustrate the potential relevance of being able to discriminate at least the most important categories. The operation of a Tokamak is restricted by several limits. The most relevant are the high-current limit, the density-limit and the pressure-limit but more empirical limits exist [3]. The current limit is typically expressed in terms of the safety factor at 95% of the plasma radius, q_{95} and operation is normally restricted to $q_{95} \geq 2$ otherwise the onset of tearing/kink instabilities can lead to a disruption. Operation at too high a density, near the so-called Greenwald-limit, can lead to a disruption due to radiation instabilities that may grow at the plasma edge. Cooling of the plasma edge contracts the plasma column reducing the value of q_{95}. Obviously this limit depends on the recycling properties of the plasma, on scrape-off layer details, on the level of impurities in the plasma edge and in general on the radiation properties of the plasma. It is worth mentioning that too low a density is also dangerous since it allows the error fields to directly penetrate the plasma and cause disruptions.

The basic pressure limit is set by the so-called Troyon limit, for which the normalized toroidal beta $\beta_N = <\beta_p>/I\ [MA]/(a[m]\ B[T])$ should be lower than ≈ 3.5. For high $q_{95} > 3$ the beta limit is only a soft limit but for $q_{95} < 3$ it tends to be more abrupt [6]. It is well known that this limit depends strongly on the peaking of the pressure and current density profiles. On JET, very fast disruptions have been seen to occur in the presence of internal transport barriers (ITBs), in the case of strongly peaked pressure profiles. These disruptions are not simple to detect because the first precursors appear a few ms before the disruption [4]. The pressure limit is often a soft limit, as operations at high β can trigger Neo-classical Tearing Modes (NTMs) that impact on the confinement and reduce the β.

On the other hand NTMs themselves can also cause disruptions. Normally tearing modes, such as NTMs, rotate with the plasma fluid. Error fields or eddy currents can cause the rotating modes to slow down and become stationary in the reference frame of the vacuum vessel, a so-called Locked Mode. After locking to the wall, the modes grow rapidly causing a disruption. The Locked Mode amplitude is one of the main signals used to predict disruptions.

Disruptions can also occur during the formation of the plasma or the ramp down of the current. A too fast plasma current ramp up results in flat current profiles (low l_i) and tends to destabilise various MHD instabilities, which can grow easily if a rational value of the safety factor is near to the plasma surface [3]. These instabilities can lock to the wall and then cause disruptions. Plasma current ramp downs at high l_i, meaning strongly peaked current profiles, are vulnerable to disruptions.

The different nature of the various causes and development of plasma stabilities, discussed above, already indicates that being able to predict not only the imminence but also the type of disruption would allow optimizing the avoidance and mitigation strategies. Some causes will lead to a very fast development of the instabilities and disruptions, while in other cases there may be ample time to act [4]. This has motivated the study reported in this paper, which is the first systematic attempt

to classify automatically the type of disruption, using a supervised clustering system based on the Geodesic distance on a manifold of Gaussian probability distributions.

The paper is structured as follows. The next section, section 2, describes the mathematics of the geodesic distance on the Gaussian manifold, assumed to represent the measurements, and how this distance can be included in both the clustering and the visualization tools developed in the rest of the paper. The database of JET discharges is described in section 3 with the discussion of the plasma quantities selected for the classification of the disruptions. Section 4 reports the results of the proposed automatic method of classification and a detailed comparison with tools based on the Euclidean distance. The last section of the paper is devoted to the summary and the description of the main developments of this line of research.

2. CLUSTERING USING GEODESIC DISTANCE ON A PROBABILISTIC MANIFOLD

In this section the geodesic distance based on the Gaussian distribution function is introduced. Its application to the clustering method developed to classify disruptions depending on their type, is also described in detail (subsection 2.1). To visualise the results, which is always an important aspect in understanding complex phenomena, the Grand Tour technique has to be upgraded to accommodate the Geodesic distance (subsection 2.2). The application of these tools to some synthetic data shows the potential of the proposed approach based on the Geodesic distance on a probabilistic manifold.

2.1 GEODESIC DISTANCE FOR CLUSTERING

The goal of any clustering algorithm is to partition a data set into groups, or clusters, such that the data are more similar to the other data of their group than to data belonging to other groups [15]. To achieve this, typically the sum-of-squares of the distances between the data and the centre of their group is minimized, but other clustering criteria can be used. In any case, the vast majority of the clustering techniques applied in practice typically are based on the assumption of a Euclidean data space. The (dis)similarity of data points are measured with the Euclidean distance, which has a precise geometrical meaning and a very long historical pedigree. However, it implicitly requires considering all data as single infinitely precise values. This assumption can be appropriate in other applications but it is obviously not the case in science, since all the measurements typically present an error bar. The idea is to develop a new distance between data, which would take into account the measurement uncertainties. The additional information provided by this distance should hopefully render the clustering algorithms to classify the data more precise. In our application this is expected to translate into a more robust automatic classification of disruption types.

The idea behind the approach proposed in this paper consists of considering the measurements not as points, but as Gaussian distributions. This is a typical assumption in plasma physics since the measurements can be in principle affected by a wide range of sources and, on the other hand, great effort are devoted to eliminating the systematic causes of errors. Each measurement can therefore be modelled as a probability density function (PDF) of the Gaussian type, determined by its mean

μ and its standard deviation σ:

$$p(x|\mu,\sigma) = \frac{1}{\sqrt{2\pi\sigma}} \exp\left[-\frac{(x-\mu)^2}{2\sigma^2}\right] \quad (1)$$

In this work, it is assumed that the mean is estimated by the value of the measurement. The standard deviation depends on the sensor and is calculated as the error bar provided by experts responsible of the various diagnostics.

Modelling JET measurements not as punctual values, but as Gaussian distributions, requires defining a distance between Gaussians. The most appropriate definition of distance between Gaussian distributions is the geodesic distance (GD), on the probabilistic manifold containing the data, which can be calculated using the Fischer-Rao metric [16]. For two univariate Gaussian distributions $p_1(x|\mu_1,\sigma_1)$ and $p_2(x|\mu_2,\sigma_2)$, parametrized by their mean μ_i and standard deviations σ_i (i = 1, 2), the geodesic distance GD is given by:

(2)

In the case of multiple independent Gaussian variables, it is easy to prove that the square GD between products of distributions is given by the sum of the squared GDs between corresponding individual distributions.

The last thing required to perform the geodesic clustering is to calculate the means of the groups. When the data are points, it is easy to calculate the mean with the Euclidean distance. Now the data are Gaussians. To calculate the mean of Gaussians, we use the hypothesis that they are independent. This implies that the sum of our Gaussian distributions, whose means are μ_1 and μ_2 and whose standard deviations are σ_1 and σ_2, is a Gaussian distribution whose mean is $\mu_1 + \mu_2$, and standard deviation $\sqrt{\sigma_1^2 + \sigma_2^2}$.

2.2 VISUALIZATION TOOLS USING THE GEODESIC DISTANCE

Visualization is always a very important ingredient in analysing complex phenomena and can be used both in the exploration phase of the data and in the final assessment of the results. In our case, visualization would be a useful tool to make sure that the clustering works correctly and also to evaluate the quality of its outputs. On the other hand, in our application, visualization is not easy since the data lay in a space of much more than 3 dimensions (see section 3). The tool chosen to visualize our data is the Grand Tour [17].

The idea implemented in the Grand Tour is to project the n-dimensional data on a set of 2-dimensional planes, so that the data is seen from "all" possible perspectives. The successive planes, referenced by a step-size t, are obtained by slight successive rotations, so that the whole n-dimensional space is approached by the planes. This being done, the sequence of planes can be plotted to visualize the complete data set.

For the benefit of the reader the essential features of the Grand Tour method are briefly described in the following. First, let's assume that the n-dimensional observed data point is A = (x_1.x_2, ..., x_n). Let us also assume that n is even: if not then we just augment each data point with a zero, to get an even number of elements. The Grand Tour performs the following tasks:

1. The program determines $n/2$ irrational numbers ω_i. A way to do this is by calculating $\omega_i = \sqrt{P_i}$, where P_i is the $i - th$ prime number. The program also determines a small positive irrational number for the step-size t.
2. The program finds two projection vectors $\alpha(t)$ and $\beta(t)$. They need to be normalized, i.e.

$$\alpha(t)^t\, \alpha(t) = \sum_{i=1}^{n} \alpha_i^2 = 1 \qquad (2)$$

$$\beta(t)^t\, \beta(t) = \sum_{i=1}^{n} \beta_i^2 = 1$$

The two projection vectors need also to be orthogonal, i.e.

$$\alpha(t)^t\, \beta(t) = 0. \qquad (3)$$

A way to satisfy these conditions is to take $\alpha(t)$ and $\beta(t)$ as

$$\alpha(t) = \sqrt{\frac{2}{n}}\,(\sin(\omega_1 Kt), \cos(\omega_1 Kt), ..., \sin(\omega_{n/2} Kt), \cos(\omega_{n/2} Kt))$$
$$\beta(t) = \sqrt{\frac{2}{n}}\,(\cos(\omega_1 Kt), -\sin(\omega_1 Kt), ..., \sin(\omega_{n/2} Kt), -\sin(\omega_{n/2} Kt)) \qquad (4)$$

For $K = 1, 2, ...$

3. The program then projects the data onto the plane spanned by these vectors.
4. It then displays the projected points.
5. It repeats from step 2 for the next value of K.

The traditional version of the Grand Tour algorithm is based on the Euclidean distance. The application described in this paper requires improving the clustering to calculate the Geodesic distance. In practice what is needed is a "geodesic version" of the Grand Tour, which in an approximate form has been implemented along the lines described in the following.

The Grand Tour projects data on axes (step 3 of the previously described algorithm). To achieve this, the Grand Tour needs a scalar product, which depends on the norm. In the case of the Euclidean distance, the scalar product between two vectors $x = (x_1, x_2, ..., x_n)$ and $y = (y_1, y_2, ..., y_n)$ is simply given by:

$$< x, y > = \sum_{i=1}^{n} x_i\, y_i \qquad (5)$$

In the case of the geodesic distance, it is possible to calculate, from the Fischer-Rao Metric, the matrix of the new scalar product, which is:

$$G_{\mu\nu} = \begin{pmatrix} \frac{1}{\sigma_i^2} & 0 & \dots & 0 \\ 0 & \frac{1}{\sigma_i^2} & \dots & 0 \\ \dots & \dots & \dots & \dots \\ 0 & 0 & \dots & \frac{1}{\sigma_i^2} \end{pmatrix} \tag{6}$$

The scalar product between x and y becomes:

$$< x \mid G_{\mu\nu} \mid y > = \sum_{i=1}^{n} \frac{x_i y_i}{\sigma_i^2} \tag{7}$$

More details on the Grand Tour based on the Geodesic distance can be found in [17].

2.3 A NUMERICAL EXAMPLE

In this section, some results, based on synthetic data, are reviewed to show the potential of the tools based on the Geodesic distance compared to their version using the Euclidean distance. First of all, 50 random 6-dimensional vectors have been generated. The data belong to five groups, with the same mean 20, but with different standard deviations: 10 vectors have standard deviation of 1, 10 vectors have standard deviation of 2, 10 vectors have standard deviation of 3, 10 vectors have standard deviation of 5 and 10 vectors have standard deviation of 7. These data are very close only their average value is taken into account, which is what the Euclidean distance does. But, if the Gaussian distribution used to generate them is taken into account, as done by the geodesic distance, they can be more easily distinguished.

To illustrate this point with the synthetic data, the results obtained with a classic K-means clustering [14] are plotted in figure 1 using the Grand Tour. The axes of the figures are two representative projection axes of the Grand Tour. Stars represent the data. The k-means groups the data in different clusters with different colours. The centres (i.e the means) of the clusters are plotted as black crosses. On the left, the groups have been generated using the geodesic distance. On the right, the Euclidean distance has been used.

The version of k-means based on the Geodesic distance manages rather well to find five distinct groups. On the contrary, the k-means fails when it uses only the Euclidean distance: the data are scattered and the groups overlap and cannot be separated. It is worth mentioning that in Figure 1 the Grand Tour has been used to visualise the clusters identified by the k-means. On the other hand also the Grand Tour alone shows the same behaviour; the version using the geodesic distance manages to better discriminate the five groups (even without the previous k-means clustering).

In order to quantify more precisely the extra value of the Geodesic distance, the Rand Index

[15] for these clusters has been calculated. The Rand Index takes values between zero and 1 and quantifies how similar two different clusterings are (1 for the highest similarity). Therefore this parameter can be evaluated to measure how similar the two obtained clusterings are to the original synthetic groups. The Rand Index between the Geodesic k-means and the original clustering is 0.94041, whereas the Rand Index between the Euclidean k-means and the original clustering is 0.69061. This means that the Geodesic k-means performs a lot better than the Euclidean k-means to retrieve the original clusters. This simple example shows that the use of the Geodesic distance permits to classify more efficiently the data when they are affected by significant noise.

3. JET DATABASE

On JET, the disruptions have always been monitored and a global database is available. For many of the disruptive shots, in addition to the time of the disruption, also the most probable root cause of the disruption is identified [4]. The results reported in this paper have been obtained considering a set of 795 non-intentional disruptions in the range between Pulse No's: 49948 and 79831. All these Pulse No's have taken place with the carbon wall and not with the new ITER-like wall; this is due to the fact that only with the old carbon wall the statistical basis is sufficient to study the various types of disruptions.

JET disruptions are typically classified by the experts in the eight groups reported in table I. This established classification allows comparing the results of the automated clustering with the expert classification. In the first group, ASD, the disruptions are mainly due to technical problems. Therefore this group of shots has not been included in the statistics reported in the following. It has been checked, however, that when these cases are included the results of the proposed methodology are not qualitatively affected.

The plasma quantities used to classify these discharges are listed in table II. The choice of these quantities is mainly due to their availability in real-time and their relation to plasma stability. A near identical set of quantities has already been used by APODIS and in any case they can be easily made available for real-time applications. These quantities have been taken every ten milliseconds in the interval between 300 and 10 milliseconds before the disruption.

4. AUTOMATIC CLASSIFICATION RESULTS

The main purpose of the work described in this section is to establish the potential of classifiers based on the Geodesic distance to outperform the ones based on the Euclidean distance. In this perspective, it has been decided to adopt supervised clustering tools and to consider the disruptive shots in the database as individual independent examples. Every shot has therefore been considered a new example to classify, on the basis of the already available clusters, formed by the remaining discharges. The other cases, different from those to be classified, have been clustered according to the classification of the experts. Therefore, in practice, for each case of the 795 in the database, the geodesic and Euclidean distance have been used to classify it in one of the clusters, obtained by

grouping the remaining 794 shots according to the expert evaluation.

A point to emphasize is that the shot under consideration is to be assigned to one of the clusters depending on the criterion selected to evaluate the similarity. Indeed in any clustering method, one needs to decide the criterion to assign a new example to the appropriate cluster. A systematic investigation has been performed to identify the most appropriate strategy. The distance to the barycentres, the mean of the distances to all the points in the various clusters have given reasonable results but the best success rate in the classification has been obtained using the nearest neighbour criterion. The new example is attributed to the cluster which contains the disruptive shot closest to the new discharge to classify. This classification has been performed with both the Euclidean and the geodesic distances. The results are reported in figure 2. Since the error bars of the measurements are not always easy to determine, the standard deviation of the Gaussians has also been varied to identify the most appropriate value.

The results are encouraging. Up to 85% of success rate, to be interpreted as the number of shots classified in the same class as the experts, has been reached about 150 ms before the disruption (before the thermal quench). The best results are obtained when the highest standard deviations are set to 2% of the measured values. The improvement with respect to same tools using the Euclidean distance is typically more than 5%. This is particularly significant since the tools using the geodesic distance outperform the ones using the Euclidean distance for all times and all types of disruption (see also later). The 85% success rate has to be compared to a random classification which would have correctly sorted one seventh of the shots, i.e. around 14% of the shots. Thus, the obtained success rate is quite satisfactory.

The success rate has also been particularised for the type of disruption. The results are shown in figure 3. Once again, the success rates are very high. Even the lowest success rate is higher than 70%, which is quite satisfactory. Moreover the classification with the geodesic distance is superior to the Euclidean distance in terms of success rate for all the types of disruptions. As expected, the group of discharges, with disruptions due to too strong and ITB, form a more distinct group (higher success rate) than those due to density control problems.

One quite general trend of the obtained results is the decrease of the success rate after abound 40 milliseconds before the disruption time. This can be explained by the change in characteristics originating from the onset of instabilities that eventually lead to the disruption. This emphasises the fact that the presented method is implemented in a way aimed at identifying the plasma scenario, in which a particular disruption type takes place, but not at predicting its onset. Whereas the simple prediction of a disruption becomes easier the closer to the disruption time, if the objective consists of the discrimination between the various types of disruption, it is advantageous to classify not too close to the thermal quench.

CONCLUSION

A novel approach for automatically discriminating disruption types has been implemented and tested

at JET using an extensive database. The method, which is compatible with real-time applications, consists of clustering the discharges using the geodesic distance on a Gaussian manifold. The nearest neighbour approach provides the best results; overall the success rate in the classification exceeds 85% and no type of disruption is classified with a success rate lower than 70%. These values are more than satisfactory since it must also be taken into account that some disruptions are very difficult to classify and therefore that also the grouping provided by the experts is certainly not absolutely correct (even if it has been considered 100% correct in the computation of the reported results).

Given the success rate already achieved, it is planned to deploy soon this method in JET real-time system. In this perspective it is worth emphasizing that the developed clustering technique it is a classification method not a prediction tool. In its present form, it basically discriminates the plasma scenario in which specific disruption types take place but does not predict the on-set of the disruptions. Therefore the approach must be combined with a predictor capable of determining sufficiently in advance the imminence of a disruption. The main strategy presently considered at JET consists of coupling the described clustering with the predictor APODIS. APODIS can indeed provide a very high success rate in predicting the occurrence of the disruptions [13]. Once an alarm has been triggered, the clustering can be performed to determine the most likely disruption type to be expected. At the moment various strategies are being investigated for the calculation of the required distances in real-time. Of course the success of the combined system also will depend on correctly predicting each of the disruption types that are discussed in this paper. The prediction success may vary per disruption type. The important improvement would be that the combined system would be able to allow different actions to a predicted disruption, depending on the type of disruption that is expected.

With regards to the issue of improving further the classification success rate, it must be considered that the quantities considered so far are the signals already available in real-time and optimised in the past for the prediction of disruption not for their classification. Therefore a different set of signals could provide much better results and this point will have to be investigated in more detail in the near future. Moreover, only the absolute values of the selected quantities have been used to classify the types of disruptions. On the other hand, for prediction, it is well known that also the frequency content of the signals can be very useful. Therefore also this aspect should be tested and see to what extent information in the frequency domain can help in discriminating the various disruptions types. In this perspective, the wavelength transform of the measurements could be considered; developing the geodesic distance method along this line is already explored in [18].

To conclude it is worth mentioning again that the developed strategy, based on the clustering using the Geodesic distance, is an interesting new development also from the conceptual point of view. In science in general, and in fusion in particular, the classification methods implemented do not take into account the error bars of the measurements. Calculating the distances on the Gaussian manifold permits to include also the uncertainties of the measurements in the final evaluation. In this perspective, it is worth mentioning that the approach is fully general and that it could be applied

successfully to other distribution models and to other problems requiring classifications of different plasma states, such as the studies of the L-H transition [19].

ACKNOWLEDGMENTS

This work, supported by the European Communities under the contract of Association between EURATOM/CIEMAT/ENEA/FOM, was carried out within the framework of the European Fusion Development Agreement. The views and opinions expressed herein do not necessarily reflect those of the European Commission

REFERENCES

[1] J. Wesson "*Tokamaks*" Oxford University Press; 2004.

[2] P. Helander, L.-G. Eriksson, A. Andersson, "*Runaway acceleration during magnetic reconnection in tokamaks*", Plasma Physics and Controlled Fusion, **44** (19xx) B247

[3] T.C. Hender, J.C. Wesley, J. Bialek, A. Bondeson, A.H. Boozer, R.J. Buttery, A. Garofalo, T.P. Goodman, RS Granetz, Y. Gribov, et al. "*MHD stability, operational limits and disruptions*" Nuclear Fusion **47** (2007) S128.

[4] P.C. de Vries, M.F. Johnson, B. Alper, P. Buratti, T.C. Hender, H.R. Koslowski, and V. Riccardo. "*Survey of disruption causes at JET*" Nuclear Fusion **51** (2011) 053018.

[5] P.C. de Vries, et al., *"Impact of the ITER-like wall at JET on disruptions"* Plasma Phys. Control. Fusion (2012) (in press)

[6] F.C. Schuller, "*Disruptions in tokamaks*" Plasma Physics and Controlled Fusion **37** (1995) A135.

[7] J.V. Hernandez, A. Vannucci, T. Tajima, Z. Lin, W. Horton, and S.C. McCool, "*Neural network prediction of some classes of tokamak disruptions*" Nuclear Fusion **36** (1996) 1009.

[8] B. Cannas, A. Fanni, E. Marongiu, and P. Sonato "*Disruption forecasting at JET using neural networks*" Nuclear Fusion **44** (2004) 68

[9] G. Pautasso, C. Tichmann, S. Egorov, T. Zehetbauer, O. Gruber, M. Maraschek, K.F. Mast, V. Mertens, I. Perchermeier, G. Raupp, et al. "*On-line prediction and mitigation of disruptions in asdex upgrade*" Nuclear Fusion **42** (2002) 100.

[10] R. Yoshino. "*Neural-net disruption predictor in JT-60U*" Nuclear fusion 43 (2003) 1771.

[11] A. Murari, J. Vega, G.A. Rattà, G. Vagliasindi, M.F. Johnson, S.H. Hong "*Unbiased and non-supervised learning methods for disruption prediction at JET"* Nuclear Fusion **49** (2009) 055028.

[12] G.A. Rattá, J. Vega, A. Murari, G. Vagliasindi, M.F. Johnson, and P.C. De Vries "*An advanced disruption predictor for jet tested in a simulated real-time environment"* Nuclear Fusion **50** (2010) 025005.

[13] J. Vega et al., *"Results of the JET real-time disruption predictor in the ITER-like wall campaigns"*. 27th Symposium on Fusion Technology. 2012 (Liège,Belgium), submitted to Fusion Technology Engineering.

[14] M. Lehnen et al., "*Disruption mitigation by massive gas injection in JET*" Nuclear Fusion **51** (2011) 123010

[15] S.Theodoridis and K.Koutroumbas "Pattern Recognition" Fourth Edition, Academic Press, London, 2009

[16] G. Verdoolaege and P. Scheunders, "*On the geometry of multivariate generalized Gaussian models*" Journal of Mathematical Imaging and Vision, **43** (2011) 180.

[17] W.L.Martinez and A.R.Martinez, "*Exploratory Data Analysis with Matlab*" CRC Press Company, 2005, London.

[18] J. Burbea and C. Rao, "*Entropy differential metric, distance and divergence measures in probability spaces : a unified approach.*", J. Multivariate Anal., **12** (1982) 575.

[19] G. Verdoolaege, G. Karagounis, A. Murari, J. Vega, G. Van Oost and JET-EFDA contributors, "*Modeling fusion data in probabilistic metric spaces: Applications to the identification of confinement regimes and plasma disruptions.*" Fusion Science and Technology 2012 (in press).

Type of disruption	Acronym
Auxiliary Power Shut – Down	(ASD)
Greenwald Limit	(GWL)
Internal Transport Barrier	(ITB)
Current Rump – Up	(IP)
Density Control Problem	(IMC)
Low Density and Low 'q'	(LON)
Neo-Classical Tearing Mode	(NTM)
Impurity Control Problem	(NC)

Table I: List of different disruption types as defined in [1] with acronyms.

Signal	Unit
Plasma Current	Amp
Plasma Density	m^{-3}
Derivative of Stored Diamagnetic Energy	Watt
Radiated Power	Watt
Mode Locked Mode Amplitude	Tesla
Total Input Power	Watt
Vertical position of the magnetic axis	m
Beta poloidal	n.a.

Table II: plasma quantities used to classify JET disruptions .

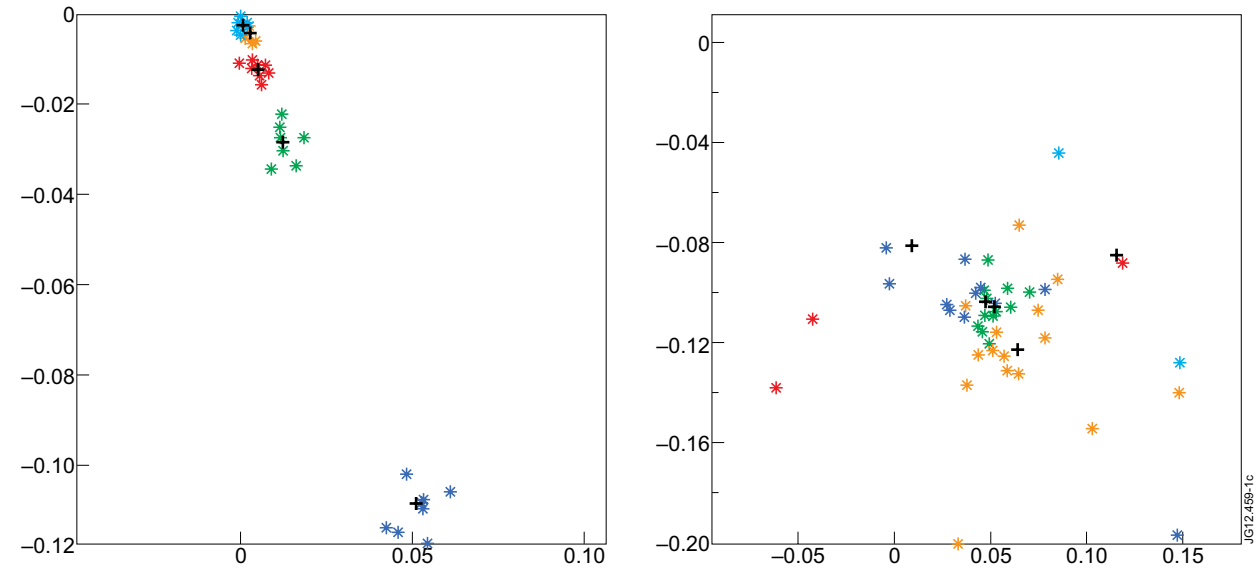

Figure 1: Grand Tour Projections for the k-means clustering of the synthetic data. Left hand plot: k-means with the Geodesic distance. Right hand plot: k-means with the Euclidean distance. The colour code of the points reflects the clustering performed by the K-means. The crosses are the barycentres of the clusters as determined by the k-means. Since this is a simple numerical example, the axes are non dimensional.

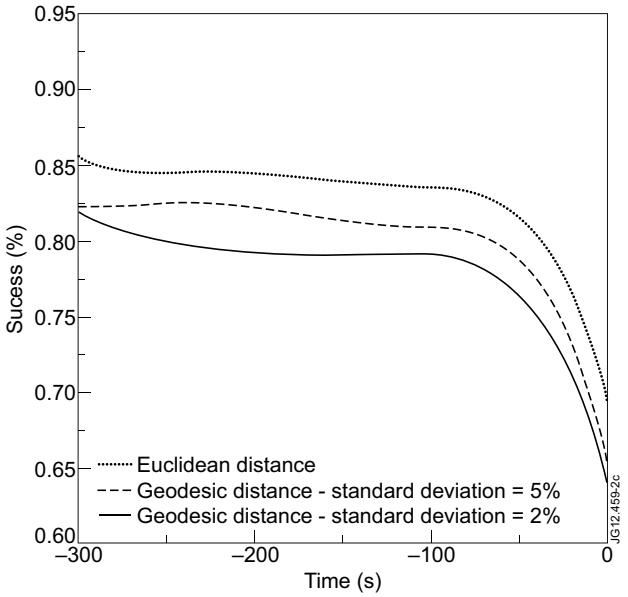

Figure 2: Percentage of well classified shots against time using the nearest neighbour method, using the geodesic distance and the Euclidean distance. In both case the ASD disruptions have been considered. The standard deviation of the Gaussian has also been varied to identify the most appropriate value.

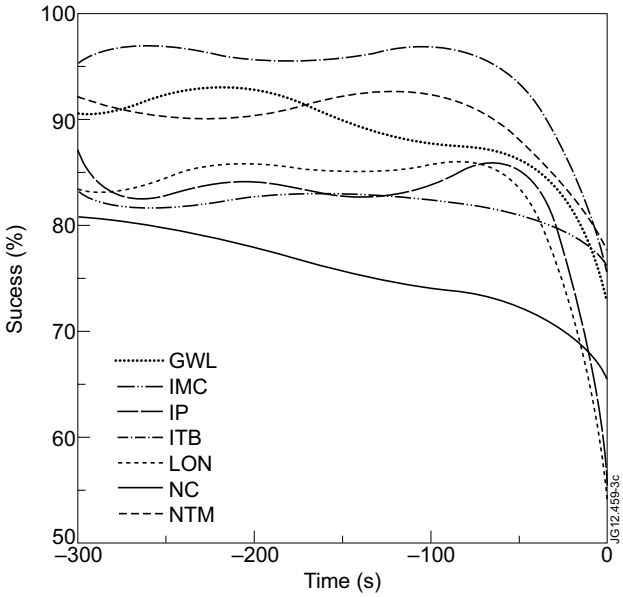

Figure 3: Percentage of well-classified shot for each type of disruption using the geodesic distance with 2% standard deviation. The y axis is the percentage of disruption of each type that the developed clustering method puts in the same class as the experts.